Molecular Pharmacology Fast Forward. Published on January 24, 2018 as DOI: 10.1124/mol.117.110627
This article has not been copyedited and formatted. The final version may differ from this version.

Title Page

Elucidation of the binding mode of the carboxyterminal region of peptide YY to the human Y_2 receptor

Authors: Bo Xu, Silvana Vasile, Søren Østergaard, Johan F. Paulsson, Jasna Pruner, Johan Åqvist, Birgitte S. Wulff, Hugo Gutiérrez-de-Terán and Dan Larhammar

Affiliations:

Department of Neuroscience, Biomedical Centre Box 593, Science for Life Laboratory, Uppsala University, SE-75124 Uppsala, Sweden. (B.X., J.P., D.L.)

Department of Cell and Molecular Biology, Biomedical Centre Box 596, Uppsala University, SE-75124 Uppsala, Sweden. (S.V., J.Å., H.G.d.T.)

Protein & Peptide Chemistry 2, Novo Nordisk A/S, 2760 Måløv, Denmark. (S.Ø.)

Obesity Research, Novo Nordisk A/S, 2760 Måløv, Denmark. (J.F.P., B.S.W.)

Molecular Pharmacology Fast Forward. Published on January 24, 2018 as DOI: 10.1124/mol.117.110627
This article has not been copyedited and formatted. The final version may differ from this version.

Running Title Page

Running Title: PYY binding to the Y_2 receptor

Corresponding Authors:

Hugo Gutiérrez de Terán
Phone: +46 18 4715056
Fax: +46 18 530396
E-mail: hugo.gutierrez@icm.uu.se

Dan Larhammar
Phone: +46 18 4714173
Fax: +46 18 511540
E-mail: dan.larhammar@neuro.uu.se

Number of text pages: 48
Number of tables: 2
Number of Fig.s: 5
Number of references: 74
Number of words in the Abstract: 245
Number of words in the Introduction: 734
Number of words in the Discussion: 1383

Supplemental data is attached

Abbreviations:
ACN: acetonitril
DIC: N,N´-diisopropylcarbodiimide
DCM: dichloromethane
DMF: N,N-dimethylformamide
FA: formic acid
Fmoc: fluorenylmethyloxycarbonyl
HOBt 1-hydroxybenzotriazole
MD: molecular dynamics
NMP: N-methylpyrrolidone
NPFF: neuropeptide FF
NPY: neuropeptide Y (for tyrosine)
PRLH: prolactin releasing hormone
PYY: peptide YY (for tyrosine-tyrosine)
PP: pancreatic polypeptide
QRFP: pyroglutamylated RFamide peptide
RP-HPLC: reverse phase high-performance liquid chromatography
RP-UPLC: reverse phase ultra-performance liquid chromatography
SPA: scintillation proximity assay
SEM: standard error of the mean
TFA: trifluoracetic acid
TIPS: triisopropylsilane
WT: wildtype

Molecular Pharmacology Fast Forward. Published on January 24, 2018 as DOI: 10.1124/mol.117.110627
This article has not been copyedited and formatted. The final version may differ from this version.

Abstract

Understanding the agonist-receptor interactions in the neuropeptide Y (NPY)/peptide YY (PYY) signaling system is fundamental for the design of novel modulators of appetite regulation. We report here the results of a multidisciplinary approach to elucidate the binding mode of the native peptide agonist PYY to the human Y_2 receptor, based on computational modeling, peptide chemistry and in vitro pharmacological analyses. The preserved binding orientation proposed for full-length PYY and five analogues truncated at the amino terminus explains our pharmacological results where truncations of the N-terminal proline helix showed little effect on peptide affinity. This was followed by receptor mutagenesis to investigate the roles of several receptor positions suggested by the modeling. As a complement, PYY-(3-36) analogues were synthesized with modifications at different positions in the common PYY/NPY C-terminal fragment (^{32}TRQRY^{36}-amide). The results were assessed and interpreted by molecular dynamics and Free Energy Perturbation (FEP) simulations of selected mutants, providing a detailed map of the interactions of the PYY/NPY C-terminal fragment with the transmembrane cavity of the Y_2 receptor. The amidated C-terminus would be stabilized by polar interactions with Gln288$^{6.55}$ and Tyr219$^{5.39}$, while Gln130$^{3.32}$ contributes to interactions with Q^{34} in the peptide and T^{32} is close to the tip of TM7 in the receptor. This leaves the core, α-helix of the peptide exposed to make potential interactions with the extracellular loops. This model agrees with most experimental data available for the Y_2 system and can be used as a basis for optimization of Y_2 receptor agonists.

Molecular Pharmacology Fast Forward. Published on January 24, 2018 as DOI: 10.1124/mol.117.110627
This article has not been copyedited and formatted. The final version may differ from this version.

Introduction

The human neuropeptide Y (NPY) signaling system consists of three peptides (NPY, peptide YY (PYY) and pancreatic polypeptide (PP)) and four receptors (Y_1, Y_2, Y_4 and Y_5) (Michel *et al.*, 1998). Cancer and obesity are among the many pathophysiological functions regulated by this neural and endocrine system (Zhang *et al.*, 2011). In particular, food intake is stimulated by NPY through activation of the Y_1 and Y_5 receptors (Fekete *et al.*, 2002; Lecklin *et al.*, 2002; Mashiko *et al.*, 2009), or inhibited through activation of receptors Y_4 (by PP) (Sato *et al.*, 2009) or Y_2 by PYY-(3-36) (Degen *et al.*, 2005; Neary and Batterham, 2009; Pedersen *et al.*, 2010), an endogenous truncated version of PYY. Consequently, many efforts have been made to develop drugs for regulating this system to treat obesity, either with Y_1/Y_5 antagonists or Y_2/Y_4 agonists (Brothers and Wahlestedt, 2010; Walther *et al.*, 2011; Yulyaningsih *et al.*, 2011). Of particular interest is the pathway regulated by the Y_2 receptor which is located in the arcuate nucleus of the basal hypothalamus. Here, stimulation by PYY-(3-36), arriving via the blood from the gastrointestinal tract, reduces release of the appetite-stimulating peptides NPY and AGRP in the paraventricular nucleus (Schneeberger *et al.*, 2014). In the search for therapeutically useful agonists to regulate this pathway, several peptides and peptidomimetics have been generated by modification of the common C-terminus of NPY/PYY peptides, which shed light on the structural determinants of high affinity and selectivity (Kirby *et al.*, 1997; Balasubramaniam *et al.*, 2000; Pedersen *et al.*, 2009; Albertsen *et al.*, 2013; Ehrlich *et al.*, 2013; Pedragosa-Badia *et al.*, 2013; Nishizawa *et al.*, 2017).

The crystallization of G-protein-coupled receptor (GPCR) structures has blossomed in the last decade (Katritch *et al.*, 2013). Still, the majority of receptors have to be investigated through computational modeling, a process that benefits

greatly from site-directed mutagenesis studies to characterize receptor-ligand binding modes (Kristiansen, 2004; Salon *et al.*, 2011; Zhukov *et al.*, 2011). In this field, our group has recently contributed with a computational protocol, based on free energy perturbation (FEP), to estimate the effects of single point mutations on ligand binding affinity with high accuracy and precision (Boukharta *et al.*, 2014; Keränen *et al.*, 2014, 2015; Nøhr *et al.*, 2017; Vasile *et al.*, 2017). The protocol was first developed and validated within the scope of the present project, in particular in the case of antagonist binding to the NPY/PYY receptor Y_1 (Boukharta *et al.*, 2014), and later applied with success to understand both agonist and antagonist binding to the A_{2A} adenosine receptor (Keränen *et al.*, 2014, 2015) and more recently to the deorphanization of the GPR139 orphan receptor (Nøhr *et al.*, 2017).

To date, there is no crystal structure of any member of the NPY-family receptor family. Instead, several homology models of the human Y_1 and Y_2 receptors have been proposed on the basis of the available experimental structures of rhodopsin-like GPCRs and assessed by mutagenesis and pharmacological studies (Sautel *et al.*, 1996; Kannoa *et al.*, 2001; Sjödin *et al.*, 2006; Merten *et al.*, 2007; Åkerberg *et al.*, 2010; Fällmar *et al.*, 2011; Xu *et al.*, 2013; Boukharta *et al.*, 2014; Pedragosa-Badia *et al.*, 2014; Kaiser *et al.*, 2015). Our most recent hY_2 model was built on the basis of the neurotensin receptor 1 (NTS_1) active-like crystal structure (White *et al.*, 2012), and verified with site-directed mutagenesis and binding studies. We showed the utility of this model to elucidate the binding mode of the C-terminal coil of the agonist peptides, ^{32}TRQRY^{36}-NH_2, in the transmembrane (TM) regions of the receptor (Xu *et al.*, 2013). Later, Beck-Sickinger and co-workers reported a different modeling approach, complemented by mutagenesis, functional profiling and NMR data (Kaiser *et al.*, 2015). The two studies are in agreement about the binding mode of the C-

Molecular Pharmacology Fast Forward. Published on January 24, 2018 as DOI: 10.1124/mol.117.110627
This article has not been copyedited and formatted. The final version may differ from this version.

terminal coil of the PYY/NPY peptides, although presenting different interaction partners for the C-terminal amidated tyrosine residue (Y^{36}-$CONH_2$).

In the present work, we refine and extend our Y_2-agonist model to the complex with the full PYY peptide, which is used as a basis to design and characterize new receptor mutants and peptide analogs exploring the binding of the conserved PYY/NPY C-terminal fragment. The binding and functional assays were complemented with FEP simulations, and the positions investigated also assessed by evolutionary comparisons of receptor sequences. Based on these results, we propose a detailed binding model of native agonist peptides to the human Y_2 receptor that should facilitate design of subtype-selective ligands.

Molecular Pharmacology Fast Forward. Published on January 24, 2018 as DOI: 10.1124/mol.117.110627
This article has not been copyedited and formatted. The final version may differ from this version.

Materials and Methods

Computational Modeling

Generation of the Y_2 receptor model in complex with PYY and analogs. Our previously reported computational model of wild-type human Y_2 receptor (WT-hY_2) in complex with NPY (Xu *et al.*, 2013) was used as a starting point in this work. Briefly, the structure of the hY_2 receptor was obtained by homology modeling using the crystal structure of rat neurotensin receptor 1 (rNTS_1, PDB code 4GRV) as a template. This template presents the advantages of belonging to the same β-branch of class-A GPCRs as the NPY receptors, and since it was crystallized with a peptidic agonist it is referred to as an active-like conformation (White *et al.*, 2012). The quality of the model was assessed with Procheck (Laskowski *et al.*, 1993), confirming the good stereochemical quality (85% residues in the most favored regions, close to the 89% value obtained for the template, rNTS_1). The docking of the NPY peptide in our homology model was done in two stages: the amidated C-terminal pentapeptide (^{32}TRQRY^{36}-NH_2, note the residue numbering on the peptide in superscript along this manuscript) was initially docked with the Induced Fit Docking (IFD) protocol in GLIDE (Sherman *et al.*, 2006) and the resulting complex was equilibrated in the membrane with our PyMemDyn protocol, for full atom molecular dynamics (MD) simulations of GPCRs (Gutiérrez-de-Terán *et al.*, 2013). The resulting pose of the C-terminal fragment was then used as anchoring point to manually dock the full NPY peptide, starting from its NMR determined structure (Monks *et al.*, 1996), by molecular superposition and energy minimization with the Schrödinger suite (Schrödinger LCC, New York, NY). We here employed this same software to generate a new complex of the Y_2-PYY structure, given the high sequence and

structural homology between the two peptides (see Supplemental Fig. 1). The truncated analogues of the PYY at the amino tail were generated from this initial Y_2-PYY complex by simply removing the corresponding residues.

Molecular dynamics (MD) simulations. The generated peptide-receptor complexes were inserted in the membrane and equilibrated under periodic boundary conditions (PBC) using the PyMemDyn protocol (Gutiérrez-de-Terán *et al.*, 2013). Shortly, the structure is automatically embedded in a hexagonal prism-shaped box of pre-equilibrated membrane of POPC (1-palmitoyl-2-oleoyl phosphatidylcholine) lipids, with the TM bundle aligned to its vertical axis. This box is then soaked with bulk water and energy minimized with GROMACS 4.6 (Hess *et al.*, 2008), using the OPLS-AA force field (Kaminski *et al.*, 2001) for both the receptor and the peptide, combined with the Berger parameters for the lipids (Berger *et al.*, 1997). The same setup is used for a 2.5 ns MD equilibration, where initial restraints on protein and ligand atoms are gradually released from 1000 to 200 kJ/mol$Å^2$, followed by a 2.5 ns run in which the 200 kJ/mol$Å^2$ positional restraint is applied only in the C-alpha trace of the protein as described in detail in reference (Gutiérrez-de-Terán *et al.*, 2013). For each of the complexes with PYY and truncated analogues, five unrestrained replica simulations of 100 ns each were then produced, under the following MD conditions: isobaric NPT ensemble using a Nose-Hoover thermostat (Nosé and Klein, 1983) with a target temperature of 310 K. Electrostatic interactions beyond a cutoff of 12 Å were estimated with the particle mesh Ewald method. Analyses of these MD runs were conducted with several GROMACS utilities, VMD (Humphrey *et al.*, 1996) and MDTraj (McGibbon *et al.*, 2015). Molecular superimpositions, trajectory visualizations, and molecular images were obtained with PyMOL. For the MD

simulations of each peptide in water, a cubic box was generated to solvate the peptide (12 Å minimum distance to the boundary) and subjected to a short equilibration, consisting on 0.1 ns in the NVT ensemble followed by 0.2 ns in NPT (constant pressure) conditions. Thereafter, five unrestrained replica simulations of 10 ns followed, under the same conditions as for the complexes.

Free Energy Perturbation (FEP) calculations. The model of the WT-hY_2 in complex with PYY (holo form) and the corresponding reference (apo form, obtained by deleting the ligand and resolvating the originated cavity) were retrieved from the previous MD equilibration under PBC. Each system was transferred to a spherical boundary system for free energy perturbation (FEP) calculations, performed with the software Q (Marelius *et al.*, 1998) using the same force field parameters described for the PBC simulations. A sphere with radius 25 Å, centered on the alpha-carbon of Q^{34} of PYY in the complex, was created. A 10 kcal/mol$Å^2$ positional restraint was applied on solute atoms within the outer shell of the sphere (i.e. 22-25 Å from the center), while solvent atoms were subjected to polarization and radial restrains, using the surface constrained all-atom solvent (SCAAS) (King and Warshel, 1989; Marelius *et al.*, 1998) model to mimic the properties of bulk water at the sphere surface. Solvent bond and angles were constrained using the SHAKE algorithm (Ryckaert *et al.*, 1977). Atoms lying outside the simulation sphere were tightly constrained to their initial positions with a 200 kJ/mol$Å^2$ force constant, and excluded from the calculation of non-bonded interactions. Long range electrostatics interactions beyond a 10 Å cut-off were treated with the local reaction field method (Lee and Warshel, 1992), except for the atoms of the sidechains involved in the FEP transformations, to which no cut-off was applied. Ionisable residues near the boundary of the sphere were

neutralized, in order to avoid artifacts due to missing dielectric screening (Åqvist, 1996), while all titratable residues outside the sphere were neutralized.

The spherical systems were equilibrated with an initial heating phase of 0.11 ns, the temperature slowly raised up from 1 K to 310 K whilst the positional restraints initially applied to the solute atoms (25 kcal/molÅ^2) were released, followed by 0.5 ns of unrestrained equilibration (for mutations involving charged residues the equilibration time was doubled) at the final constant temperature of 310 K (bath coupling of 0.1 fs) with a time step of 1 fs. MD sampling under the same conditions followed, accounting for the sampling for FEP calculations. Data collection consisted of 10 replica simulations, each starting with different random velocities, for each simulated state (i.e., *apo* and *ligand-bound* receptor). Each independent simulation lasted for 4-7 ns (depending on the mutation), leading to a total sampling time of 2 (states) x 10 (replicates) x [4-7] (ns/replica/state) ≈100 ns per simulated mutation. The standard error of the mean (SEM) was reported for each case based on the statistical analysis of the 10 replicate simulations. Our FEP protocol for amino acid mutations has been described elsewhere (Boukharta *et al.*, 2014; Keränen *et al.*, 2014, 2015). Briefly, a given mutation of any residue to alanine was divided in several smaller subperturbations to allow for a smoother transition between the end-states. Three steps were introduced for groups of atoms (charge groups) starting with the group with the highest topological distance (number of atoms) from the protein backbone: i) removal of partial charges per charge group, ii) introduction of a soft core van der Waals potential and iii) full annihilation of the involved atom(s). The last step included the introduction of the Cβ hydrogen atom of the alanine residue. For non-alanine mutations, initial models of mutant receptors were created with PyMol, using the most probable rotamer of the mutated residue, and a double thermodynamic cycle

Molecular Pharmacology Fast Forward. Published on January 24, 2018 as DOI: 10.1124/mol.117.110627
This article has not been copyedited and formatted. The final version may differ from this version.

was joined (i.e., WT -> Ala and mut -> Ala), meaning that in these cases double simulation time was needed (i.e., ~200 ns per mutation) and that the associated SEM is expected to go above the 1 kcal/mol value typical of Ala mutations (Boukharta *et al.*, 2014; Keränen *et al.*, 2014, 2015). For mutations of charged residues, a counter ion (chloride for mutation of Glu, potassium for Arg mutations) was placed in the bulk solvent, partially restrained and simultaneously charged, to maintain the total charge of the sphere constant along the FEP transformation. In these cases, the heating and the equilibration times were doubled and the sidechain of the mutated residue was constrained to its initial position with 5 kcal/mol$Å^2$ during the equilibration phase to increase the convergence of the simulations. In order to compare with the experimental mutant binding data, we converted the experimental K_i values into $\Delta\Delta G$ using:

$$\Delta\Delta G^{mut} = RTln\frac{K_i^{mut}}{K_i^{wt}}$$

Mutagenesis

The primers for the mutagenesis were designed using web-based software PrimerX (http://www.bioinformatics.org/primerx/) and synthesized by Eurofins Genomics (Ebersberg, Germany) and purified with high pure salt free method. The QuikChange II site-directed mutagenesis kit (Agilent Tachnologies, Santa Clara, CA, USA) or AccuPrime Pfx SuperMix (Thermo Fisher Scientific, Waltham, MA, USA) was used for introducing mutations to the human Y_2 receptor (WT-hY_2, UniProt P49146) coding region inserted in a pcDNA-DEST47 vector (Thermo Fisher Scientific, Waltham, MA, USA,) according to manufacturer's protocols. The

generated PCR product was transformed into One Shot® Top10 *E.coli* cells (Thermo Fisher Scientific, Waltham, MA, USA). The Y_2 receptor mutations were confirmed by sequencing of the whole Y_2 coding region (Eurofins). The plasmids containing different mutations were purified with Pulink plasmid purification kit (Thermo Fisher Scientific, Waltham, MA, USA) eluted in pure water and stored at -20°C for future transfections.

Membrane preparation

HEK293 cells were grown on 55 cm^2 Nunclon cell culture dishes (Thermo Fisher Scientific, Waltham, MA, USA) to 90-95% confluency and transfected with Y_2 wild type or mutant plasmids. After 72 hours, plates were washed in ice cold Phosphate-buffered saline (PBS), and scraped mechanically from the plates. The cells were then transferred to tubes and centrifuged for 5 min at 1000 g. Pellets were resuspended in ice cold binding buffer (25 mM HEPES, 2.5 mM $CaCl_2$, 1.0 mM $MgCl_2$ and 0.2% Bacitracin, pH 7.4) used for binding assays described below and then homogenized for 30 seconds using an Ultra-Turrax homogenizer at medium speed. The homogenate was centrifuged at 3500 g for 5 min, the supernatant was discarded and fresh cold buffer was added. Homogenization of the pellet was repeated three times. The final pellet was resuspended in binding buffer to 1 ml and stored at -80 °C.

Synthesis of PYY and its analogues

All chemicals were of analytical grade or higher. Triisopropylsilane (TIPS), N,N´-diisopropylcarbodiimide (DIC), acetic anhydride, thioanisole, collidine and

formic acid (FA) (≥98%) were from Sigma‑Aldrich, Chemie GmBH (Steinheim, Germany). Acetonitrile (ACN), dichloromethane (DCM) (LiChrosolve), trifluoroacetic acid (TFA), and diethyl ether were purchased from Merck KGaA (Darmstadt, Germany). Water came from a MilliQ equipment (Advantage A10) from Millipore (Molsheim, France). 2-Chlorotrityl chloride polystyrene, Rink-amide or PAL polystyrene resins were purchased from Merck KGaA (Darmstadt, Germany). Standard Fmoc amino acids, resins and coupling reagents, 1-hydroxybenzotriale (HOBt) and OxymaPure Novabiochem® were from Merck KGaA (Darmstadt, Germany) or Protein Technologies (Tucson, USA). N-Methylpyrrolidone (NMP) dimethylformamide (DMF) and piperidine were from Biosolve (Dieuze, France).

Peptide analogues (see Supplemental Fig. 2) were prepared using a Prelude or Prelude X peptide synthesizer (Protein Technologies, Tucson, Arizona US) using a Fmoc-chemistry protocol for solid phase peptide synthesis and either Fmoc-Rink-amide or Fmoc-PAL polystyrene resins. Each coupling used 6‑8 eq. Fmoc-amino acid-OH and OxymaPure in DMF (both 6-8 eq.) and activated by DIC and collidine also both 6-8 eq. The amino acid solutions were all 0,3 M containing also 0,3 M OxymaPure. The DIC and collidine solutions were both 3 M and added as 1/10 volume compared to the volume of Fmoc-amino acid solutions. For deprotection of Fmoc, 25% piperidine in NMP or DMF was used for 4 + 4 min (or 2+ 2 min using heating 55 ^{o}C on Prelude X). Coupling time was set to 60 min (or 30 min using heating 45-55 ^{o}C on Prelude X) while double coupling was performed for Fmoc-Arg(Pbf)-OH and a total coupling time of 1 h (or 20 + 40 min using heating 55 ^{o}C on Prelude X).

Synthesis of PYY-(3-36) methylamide was done using the linker (3-formylindolyl)acetamidomethyl polystyrene (Merck Millipore) from Epstep (Estep,

Neipp et al. 1998). Coupling of Fmoc-Tyr(Otbu)-OH onto this linker was done using 8 eq, 8 eq DIC and 8 eq OxymaPure in DMF and heating at 55 ^{o}C for 2 hours. After coupling the resin was capped using 10 eq acetic anhydride in DMF for 30 min.

Synthesis of PYY-(3-36)-ol (the C-terminal as primary alcohol) was done by coupling 5 eq of Fmoc-(*O*-tert-butyl)-tyrosinol in DCM containing 3% DPEA to 2-chlorotrityl chloride polystyrene resin for 5 hours at room temperature. Coupling of residues 1-35 for both of the above analogues was done by standard SPPS Fmoc-chemistry.

Peptides were cleaved and deprotected with TFA/TIPS/thioanisole or TFA/TIPS/H_2O (95:3:2) for 1–3 h and precipitated with diethyl ether. After washing with diethyl ether 4-5 times through a 0.45 μm filter or by centrifugation, the peptides were dried. The peptides were purified by preparative RP-HPLC using a linear gradient: 15-40% ACN with 0.1% TFA over 40 min on a SymmetryPrep C18 19 × 300 mm, 7 μm column (Waters Corporation, Milford, USA) eluting at 20 ml/min. The purity of peptides was determined by analytical RP-UPLC on a Waters Acquity UPLC System with a Waters BEH column C18 using 0.05% TFA in H_2O (solvent A1) and 0.05% TFA in ACN (solvent B1). Molecular weights were determined using matrix-assisted laser desorption and ionization time-of-flight mass spectroscopy, recorded on a Microflex or Autoflex (Bruker Daltonics, Bremen,Germany). A matrix of α-cyano-4-hydroxy cinnamic acid was used. Alternatively, characterization was performed by UPLC–MS on a setup consisting of a Waters Acquity UPLC system connected to a LCT Premier XE mass spectrometer from Micromass, or by HPLC–MS on an Agilent 1200 series HPLC connected to an Agilent 6230 time-of-flight (TOF) system using 0.02% TFA in MilliQ (solvent A2) and (0.02% TFA in ACN (solvent B2). The purified analogues were dissolved in 80% DMSO with 20% H_2O as

stock solutions to a final concentration of 200 μM as quantified using a chemiluminescent nitrogen detector and RP-UPLC.

Binding assays

^{125}I-porcine PYY (^{125}I-pPYY) was used as radioligand with a specific activity of 2200 Ci/mmol (PerkinElmer, Waltham, MA, USA). Two different binding methods were used in this study: a filtration method and a scintillation proximity assay (SPA). The same binding buffer was used for both binding methods: 25 mM HEPES, 2.5 mM $CaCl_2$, 1.0 mM $MgCl_2$ and 0.2% Bacitracin, pH 7.4. Both the saturation and competition experiments were performed in U-bottom flexible 96-well plates (PerkinElmer, Waltham, MA, USA) in a final volume of 100 μl or 200 μl and incubated for 3 hours at room temperature. All binding studies were performed in duplicate and repeated independently at least three times. The saturation experiments were carried out using serial dilutions of radioligand, ^{125}I-pPYY, whereas the competition experiments were performed with serial dilutions of the competing ligand and a constant concentration of radioligand, 50 pM. In both types of binding experiments, non-specific binding was defined in the presence of 100 nM hPYY.

For the filtration method, the incubation was terminated by filtration with ice cold 50 mM Tris (pH 7.4) at 4 °C through Filtermat A GF/C filters (PerkinElmer) pre-soaked in 0.3% (v/v) polyethyleneimine (Sigma-Aldrich) using a Tomtec cell harvester. The filters were dried at 50 °C, then covered with MeltiLex scintillator sheets (PerkinElmer). For the SPA based assay, 0.5 mg/well wheat germ agglutinin SPA beads (PerkinElmer) was used and the assays were terminated by centrifugation at 500 g for 10 minutes. Light emission from scintillation beads or filters was measured using a Wallac 1450 Microbeta counter (PerkinElmer). Each assay was

optimized by adding a suitable amount of receptors, and in each case the dilution factor was determined empirically by performing test binding assays where we checked that less than 10% of the radioligand was bound.

Inositol phosphate accumulation assay

For the mutants with low expression level or too low binding affinity, a functional signal transduction assay was performed. The assay was performed according to previous descriptions (Xu *et al.*, 2013). Briefly, each receptor construct was transfected into HEK293 cells using Lipofectamine 2000 (Thermo Fisher Scientific), together with a chimeric G protein construct that changes the signaling pathway from Gi to Gq (Kostenis, 2002). Myo2-^{3}H-inositol (PerkinElmer) at 3 μCi/mL was added the day after transfection. On the third day, the cells were detached from plates after incubation with PBS/EDTA mixture (0.2 g/L) and resuspended in assay buffer with 10 mM LiCl, 20 mM Hepes, 137 mM NaCl, 5 mM KCl, 0.44 mM KH_2PO_4, 4.2 mM $NaHCO_3$, 1.2 mM $MgCl_2$, 1 mM $CaCl_2$, and 10 mM glucose. After 10 min pre-incubation, the cells were stimulated with serial dilution of peptides for 25 min at 37 °C. The cells were lysed for 60 min at 4 °C with an equal volume of 0.8 M perchloric acid, and then neutralized with $KOH/KHCO_3$ solution. Ion exchange chromatography on AG 1-X8 resin (Bio-Rad) was used to collect the generated ^{3}H-inositol phosphates. The resin was washed with buffer containing 5 mM $Na_2B_4O_7$ and 60 mM NH_4-formate and eluted with buffer containing 1 M NH_4-formate and 0.1 M formic acid. Then the samples were mixed with OptiPhase HiSafe (PerkinElmer Waltham, MA, USA) and the ^{3}H radioactivity was measured with a Tri-Carb 2910TR liquid scintillation counter (PerkinElmer Waltham, MA, USA). The

Molecular Pharmacology Fast Forward. Published on January 24, 2018 as DOI: 10.1124/mol.117.110627
This article has not been copyedited and formatted. The final version may differ from this version.

assays were performed in triplicate for each concentration and repeated at least 3 times.

Data analysis

The pharmacology assay results, K_d from saturation assay, K_i from competition assay and EC_{50} values from functional assay, were calculated with the GraphPad Prism 5.0 software using non-linear regression curve fitting function. The data were presented as geometric mean with 95% confidence interval. K_d values were determined with either filtration or SPA methods, and used to calculate the K_i values from the assays. The statistical analyses of pK_i, and pEC_{50} were performed using one-way ANOVA with Dunnett (Table 1, Table 2) or Tukey (Fig. 3) post hoc tests.

Molecular Pharmacology Fast Forward. Published on January 24, 2018 as DOI: 10.1124/mol.117.110627
This article has not been copyedited and formatted. The final version may differ from this version.

Results

MD simulations and binding affinities of PYY-(3-36) and truncated analogs

The affinities of full-length PYY and its four truncated analogues [PYY-(3-36), PYY-(18-36), PYY-(19-36) and PYY-(22-36)] for the wild-type human Y_2 receptor (WT-hY_2) are summarized in Table 1. To facilitate the analysis, the relative fold in affinity is depicted taking as a reference the K_i value of the endogenous agonist PYY-(3-36). Full-length PYY binds with about 7-fold higher affinity than PYY-(3-36), with both of these native agonists displaying affinities in the subnanomolar range (Table 1). Further truncations up to position 19 showed modest (less than 5-fold) reduction in affinity. Removal of the first 21 amino acids had a more dramatic effect with 25-fold affinity loss as compared to PYY-(3-36).

In order to characterize the peptide-receptor interactions at the structural level, we used our previously published structure of the Y_2-NPY complex as a starting point (Xu *et al.*, 2013). According to this model, the interaction network for the amidated C-terminal pentapeptide fragment (^{32}TRQRY^{36}-NH_2) is defined within the TM cavity, which was later recognized by an independent study that measured receptor potency, not affinity (Kaiser *et al.*, 2015). The characteristic secondary structure common to the NPY/PYY/PP peptides consists of a α-helix (positions 13-31), which protrudes out in the extracellular loop (EL) region, and is followed by a proline-rich helix (positions 1-12) that interacts through several H-bonds with the α-helix domain. Subsequently, we built an initial model of the Y_2-PYY complex by replacing the varying amino acids between NPY and PYY peptides, and used this as a basis to build the complexes of Y_2 with the four N-terminal truncated analogues of PYY described above. Each complex was subjected to five MD simulations of 100 ns each, where we

analyzed the stability of the complex and characterized the main interactions of the common C-terminal fragment. These interactions are well preserved and show high stability, with the residues involved in the peptide – receptor interactions being essentially the same in all five cases (see Fig. 1 and Supplemental Table 1). The slight differences in the particular peptide-receptor interactions between some peptides are not statistically significant and can thus be related to the dynamic nature of peptide-receptor binding.

However, we noted that the folding of the secondary structure elements described above (α-helix and proline helix domains) is maintained stable only in the case of PYY and PYY-(3-36). In contrast, for the shorter peptides (PYY-(18-36), PYY-(19-36) and PYY-(22-36)) misfolding of the helical part of the peptides is consistently observed (see Supplemental Fig. 3). In order to determine if this was due to the particular environment of the modeled receptor binding site, analogous MD simulations of all the five peptides were performed in water. The same trend was observed in solution, i.e., PYY and PYY-(3-36) maintain the typical interactions between the proline-rich helix and the central α-helix, whereas for the shorter peptides lacking the proline-rich helix and part of the α-helix, the remaining fragment of the α-helix is less stable (see Supplemental Fig. 4). The progressive loss in the stability of the secondary structural elements of the truncated peptides might be related to the moderate to a high decrease in binding affinity for the Y_2 receptor described above (Table 1).

Rational design and binding affinities of hY_2 receptor mutants and PYY-(3-36) analogs

Molecular Pharmacology Fast Forward. Published on January 24, 2018 as DOI: 10.1124/mol.117.110627
This article has not been copyedited and formatted. The final version may differ from this version.

As presented above, the interactions of the ^{32}TRQRY^{36}-NH_2 C-terminal fragment with the receptor are quite preserved, and the statistics on the H-bond interactions involved in this binding mode are summarized in Supplemental Table 1. Since this fragment is common to all truncated peptides and also involves a conserved region between the three peptides of the NPY family, we focused on a further characterization of the interaction pattern here proposed by comparison with available mutagenesis data, and rational design of new mutagenesis experiments, as summarized in Fig. 2. The effects on PYY-(3-36) affinity of previously investigated mutants for some of these positions are noted as a fold change in binding affinity as compared to the WT-hY_2 receptor values, while the new positions selected for mutagenesis studies are indicated. Table 2 shows the effect on PYY-(3-36) affinity (or potency, in a few indicated cases) for each of the mutants generated. To further characterize some of the binding motifs proposed, we complemented the receptor mutagenesis studies with the generation of a number of PYY-(3-36) derivatives, which include mutation of certain peptide positions to natural amino acids, plus chemical modifications of the amidated C-terminus (Fig. 3 and Supplemental Table 2).

The first group of residues selected for mutagenesis was predicted to surround T^{32} in PYY (and NPY), namely Tyr303$^{7.31}$ and Phe307$^{7.35}$ (the numbering of receptor residues is followed by the Ballesteros-Weinstein topological position commonly used for GPCRs, in superscript) (Ballesteros and Weinstein, 1995). Tyr303$^{7.31}$Ala has a negligible effect on binding affinity, while Phe307$^{7.35}$Ala importantly decreases the affinity of PYY-(3-36) (45-fold as compared to the WT-hY_2). One of the differences of our model as compared to that recently reported by Kaiser *et al.* is an interaction proposed between Tyr110$^{2.64}$ and T^{32} in the latter (Kaiser *et al.*, 2015). Therefore, we

Molecular Pharmacology Fast Forward. Published on January 24, 2018 as DOI: 10.1124/mol.117.110627
This article has not been copyedited and formatted. The final version may differ from this version.

further evaluated the effect of the Tyr110$^{2.64}$Ala mutation on peptide binding in our present model, which was found to have only a minor effect (Table 2). The peptide modification T^{32}A affected binding to the WT and mutagenized receptors, as shown in Fig. 3 and Supplemental Table 2. The affinity for WT-hY$_2$ is considerably reduced (53-fold), an effect that is mostly recovered when this peptide analogue binds to the Tyr110$^{2.64}$Ala receptor mutant and, to a lesser extent, to the Tyr303$^{7.31}$Ala mutant. Conversely, the same (T^{32}A)-PYY-(3-36) peptide shows essentially the same affinity for the Phe307$^{7.35}$Ala receptor mutant than for the wild-type. Substitution by the bulkier Phe (T^{32}F) in the peptide has a milder effect on the affinity both for the WT receptor and for the Tyr303$^{7.31}$Ala and Phe307$^{7.35}$Ala mutants, while showing slightly less affinity for the Tyr110$^{2.64}$Ala receptor than the (T^{32}A)-PYY-(3-36) peptide analogue (Fig. 3 and Supplemental Table 2).

Continuing along the peptide sequence we find a pattern of interactions for R^{33} and R^{35} that was already identified in our previous model (Xu *et al.*, 2013). These two arginines form salt bridges with Asp292$^{6.59}$ and Glu205$^{5.24}$ (in EL2), with additional contacts between R^{35} and Gln288$^{6.55}$. This interaction pattern is supported by previous mutagenesis of Asp292$^{6.59}$ to Glu, Asn, or Ala (Merten *et al.*, 2007), and of Glu205$^{5.24}$ to Ala (Merten *et al.*, 2007) or Arg (Xu *et al.*, 2013), all of which reduce agonist binding or potency. We have further complemented these mutational data with a substitution by a flexible but apolar sidechain, i.e. Glu205$^{5.24}$Leu, which had a similar effect on agonist binding (Table 2). To further assess the conformation of the EL2 region in our model, we also tested the effect of alanine mutations of Arg187$^{4.64}$ and Glu188$^{4.65}$, both of which are in the distal part of EL2 (close to TM4) and predicted to be in the vicinity of Glu205$^{5.24}$. The moderately negative impact on binding affinity when removing the positively charged Arg is in agreement with its possible role in

Molecular Pharmacology Fast Forward. Published on January 24, 2018 as DOI: 10.1124/mol.117.110627
This article has not been copyedited and formatted. The final version may differ from this version.

stabilizing the negative charge of Glu205$^{5.24}$. In the same trend is the slight gain in affinity when removing the negative charge of Glu188$^{4.65}$. Although not forming a stable interaction in our MD simulations, the initial model also suggested a role for Ser220$^{5.39}$ in an H-bond with this arginine, which would indeed be supported by the moderate decrease in binding affinity for the corresponding Ala mutation (see Table 2).

The other position in contact with R^{35} is Gln288$^{6.55}$. The previously reported conserved mutation Gln288$^{6.55}$Asn did not reduce affinity (Xu *et al.*, 2013). However, the fact that this position is also predicted to interact with the amidated C-terminal residue motivated us to explore this position by introducing less conservative replacements (see below). The peptide sidechain of glutamine Q^{34}, located between the two arginines, shows hydrogen bonds with Gln130$^{3.32}$ and Thr111$^{2.65}$ in our model. We investigated the latter side chain, and the results indicated that the corresponding alanine mutation considerably reduces the affinity (33-fold, Table 2), while Thr111$^{2.65}$Leu had a negligible effect suggesting an unspecific, non-polar interaction for the native Thr (Table 2). However, removing the polarity of the peptide sidechain (Q^{34}L mutant, Fig. 3 and Supplemental Table 2) results in a moderate loss of affinity for WT-hY_2, only slightly recovered when combined with the Thr111$^{2.65}$Leu receptor mutant. The polar interaction of Q^{34} with Gln130$^{3.32}$, on the other side, is supported by the decrease in affinity reported for its corresponding His and Glu mutants ((Xu *et al.*, 2013), see Fig. 2). To further test the role of residues in TM3 in ligand binding, we evaluated the effect of breaking the predicted proline kink provided by Pro127$^{3.29}$, which would be important to create the binding cavity needed for Y^{36} and Q^{34} (see Fig. 2). The results support this model, as Ala and especially Leu mutants have a great impact on ligand potencies determined in functional assays (Table 2).

The amidated C-terminal residue of all agonist peptides is Y^{36}. The phenol sidechain of this residue shows in our model van der Waals and H-bond interactions with Leu284$^{6.51}$ and Gln288$^{6.55}$, respectively, while the -NH_2 of the amidated C-terminus can form H-bonds with Gln288$^{6.55}$, Ser223$^{5.42}$, Tyr219$^{5.38}$ and His285$^{6.52}$ (Supplemental Table 1). Previously reported alanine mutants of Leu284$^{6.51}$ and Tyr219$^{5.38}$ showed a moderate effect on agonist binding ((Xu *et al.*, 2013) and Fig. 2). While the Tyr219$^{5.38}$Leu mutant also maintained this trend ((Xu *et al.*, 2013) see Fig. 2), we found that in the case of Leu284$^{6.51}$Tyr the binding affinity is recovered, and even increased as compared to WT-hY_2. Mutations of Ser223$^{5.42}$Ala, Ser223$^{5.42}$Leu and His285$^{6.52}$Phe showed a negligible effect on binding affinity, thus not supporting the predicted H-bonds with the peptide. Finally, the binding site of Y^{36} is optimally delimited by Cys103$^{2.57}$ in TM2, a model that is in agreement with the big decrease in ligand potency observed after the introduction of a bulky side chain in the Cys103$^{2.57}$Phe mutant (Table 2).

As for the role of the conserved Gln288$^{6.55}$, the previously reported negligible effect of a conservative Asn mutation ((Xu *et al.*, 2013) and Fig. 2) was here complemented with mutations to Ala, Leu, and Glu, all of which showed negligible to small effects in agonist binding (Table 2), whereas the introduction of a bulkier sidechain with a positive charge in the Gln288$^{6.55}$Arg showed a dramatic 79-fold reduction in the affinity of PYY-(3-36) (see Table 2). Finally, we complemented the mutagenesis exploration with other residues that in our model would be in contact with the α-helical part of the peptide. Given the minor or negligible effects on ligand binding and the difficulty in interpreting the anticipated indirect effects from mutations in this area in the absence of a crystal structure, we summarize these results in Supplemental Table 3.

The intriguing role of the amidated C-terminus in ligand binding was here further explored with the characterization of three peptide analogs that involved modifications of the amide group with a carboxylate (introducing a negative charge), a primary alcohol (removal of the carbonyl group) or methylamide (adding a methyl to amid nitrogen), all of which showed a dramatic loss of affinity (Fig. 3 and Supplemental Table 2). The methylamide analogue was further tested against mutated versions of the receptor that in principle should allow the accommodation of the bulkier methyl-amide, i.e. Tyr219$^{5.38}$Ala and Gln288$^{6.55}$Ala: the affinity was not regained, but was decreased even further. In an attempt to explore polar contacts with a positively charged Arg, double mutants of PYY-(3-36)-CH_2OH-Gln288$^{6.55}$Arg and PYY-(3-36)-COOH-Gln288$^{6.55}$Arg were also tested but showed the same negative trend.

In silico evaluation of site-directed mutagenesis with Free Energy calculations

In a final iteration, we went back to our structural model of the Y_2-PYY complex to interpret the results of the mutagenesis and functional results. Most of the interactions were initially proposed based on similar structural models by us (Xu *et al.*, 2013) and others (Kaiser *et al.*, 2015) and showed good agreement with the results of the specifically designed mutations. The interaction pattern of the amidated C-terminus in our models remained more variable (see Supplemental Table 1), which is in contrast with the tight interaction of this group with Gln130$^{3.32}$ proposed by the Beck-Sickinger group (Kaiser *et al.*, 2015). We therefore computed the effect of selected point mutations on the binding free energy of the common C-terminal fragment of agonist peptides. In particular, mutations of the positions proposed to bind the amidated C-terminus, namely Gln130$^{3.32}$, Gln288$^{6.55}$ and Tyr219$^{5.38}$, were

simulated with our recently proposed MD/FEP protocol (Boukharta *et al.*, 2014; Keränen *et al.*, 2015) and the results compared to the experimental values extracted from this work and from our previous study (Xu *et al.*, 2013). As shown in Fig. 4 and Supplemental Table 4, the calculated relative binding free energies are in good agreement with the experimental values, with mean absolute error of 1.3 kcal/mol and an average SEM of 1.47 kcal/mol (which drops to 1.16 kcal/mol if we exclude the unconverged Gln288$^{6.55}$Glu data point, see below).

Removal of the polar side chain of glutamine in the Gln288$^{6.55}$Ala mutant is found in our model to have a very small impact on peptide affinity, thereby providing a structural as well as an energetic explanation for the experimental negligible effect of this mutation. We observed an insertion of a water molecule in the Ala mutant allowing retention of the interactions with Y^{36}, partially counterbalancing the effect of the mutation. This water-mediated interaction is not stable, which is reflected in the slight over-prediction of the experimental data. Notably, the small to negligible effect in our experimental studies for mutations to sidechains that maintain the bulkiness (Leu) or the polarity (Asn) of the WT Gln, is perfectly reproduced in the FEP simulations. The same applies for the mutation to the negatively charged Glu, though in this case the simulations did not properly converge as indicated by the high associated error (Supplementary Table 4), due to the different ways of reorganization of the binding site to accommodate this negative charge. These effects are in stark contrast with the dramatic reduction of peptide affinity observed upon mutation to a longer and positively charged sidechain of Arg, which is reproduced (although overpredicted) in our model. The model indeed provides a structural interpretation of this effect, as the Arg mutation perturbs dramatically the interactions with the neighboring positively charged residues in the peptide (R^{33} and R^{35}).

Molecular Pharmacology Fast Forward. Published on January 24, 2018 as DOI: 10.1124/mol.117.110627
This article has not been copyedited and formatted. The final version may differ from this version.

As outlined above, the amino group of the C-terminal amide would mostly interact with Tyr219$^{5.38}$ in our model, which makes the most important difference with previous suggestions of an amide-amide interaction with the sidechain of Gln130$^{3.32}$ (Kaiser *et al.*, 2015). In our model, this residue would be involved in interactions with Q^{34} and the peptide backbone. Notably, the FEP simulations based on our 3D-structure of the Y_2-PYY complex perfectly explain the experimental effect of mutations of these two sidechains. Replacement of Gln130$^{3.32}$ with a negatively charged Glu or a neutral histidine is detrimental for peptide binding in both cases. A similar effect is observed and correctly reproduced when removing the sidechain of Tyr219$^{5.38}$ (mutation to Ala), an effect that is less pronounced both experimentally and in our calculations with the introduction of a bulky, hydrophobic chain (Leu). As shown in Fig. 4, the calculated relative binding free energies are in good agreement with the experimental drop in affinity for all 9 mutants, a remarkable result considering that the random probability of such a qualitative agreement is as low as $(1/2)^9 = 0.002$. Moreover, the scatter plot for the remaining 8 mutations (calculated versus experimental free energy shifts, Supplemental Figure 5) shows a good quantitative correlation, with a Pearson correlation coefficient of 0.63, which goes up to 0.85 (statistical significance for the correlation of $p < 0.005$) if we leave out the aforementioned overpredicted data point in our model Asn288$^{6.55}$Arg. Thus, our computational modeling provides further support for the network of interactions proposed herein for the ^{32}TRQRY^{36}-NH_2 peptide fragment, including the hydrogen bonding of the carboxyterminal amide with Tyr219$^{5.38}$ while Q^{34} makes contacts with Gln130$^{3.32}$.

Alignment of NPY receptors and RFamide receptors

Molecular Pharmacology Fast Forward. Published on January 24, 2018 as DOI: 10.1124/mol.117.110627
This article has not been copyedited and formatted. The final version may differ from this version.

It has been proposed that the NPY family receptors and the RFamide receptors for NPFF and PRLH, as well as QRFP (Elphick and Mirabeau, 2014; Larhammar *et al.*, 2014; Yun *et al.*, 2014), share a common ancestor from which they arose by gene duplications followed by sequence divergence. The conservation of the carboxy terminus of the peptides, with RYamide for the NPY family and RFamide for the others, correlates with a critical role of the carboxy terminus for receptor interactions for all of these receptors (Beck-Sickinger *et al.*, 1994; Mauduit *et al.*, 1998; Roland *et al.*, 1999; Boyle *et al.*, 2005; Le Marec *et al.*, 2011; Findeisen *et al.*, 2012). This should be reflected by a corresponding conservation of receptor residues that are critical for binding of the carboxy terminus of the respective peptides. Therefore, alignment of NPY receptor subtypes with RFamide receptors across vertebrates has been a constant frame of reference throughout this work. The receptor positions that we have investigated in human Y_2 are marked in the alignment with other human NPY receptor subtypes and human RFamide receptors shown in Fig. 5. We have also made alignments with all of these receptors across vertebrates. The Y_2 receptor residues proposed to interact with ^{32}TRQRY^{36}-NH_2 indeed show high conservation among the RY/RFamide receptors. The following positions are almost completely conserved among the NPY-family receptors in human and many other vertebrates: Thr111$^{2.65}$ (Val in Y_5), Gln130$^{3.32}$, Glu205$^{5.24}$ (Asp in human Y_1), Tyr219$^{5.38}$, Leu284$^{6.51}$, Asp292$^{6.59}$, Phe307$^{7.35}$, and His311$^{7.39}$. Among these, positions 2.65 and 7.35 and 6.55 differ in all RFamide receptors in comparison with the NPY-family receptors, (Fig. 5) which may explain the relative tolerance of mutations at these positions in the Y_2 receptor.

Molecular Pharmacology Fast Forward. Published on January 24, 2018 as DOI: 10.1124/mol.117.110627
This article has not been copyedited and formatted. The final version may differ from this version.

Discussion

In this study, we used a combination of experimental, evolutionary and theoretical approaches to provide a detailed map of interactions between the C-terminus of NPY/PYY and the human Y_2 receptor. Taking as a starting point our recently reported computational model of the Y_2-agonist (NPY) complex (Xu *et al.*, 2013), we initially investigated through MD simulations the interactions of Y_2 with the peptide PYY and four truncated analogs on the N-terminus. Due to the intrinsic difficulty in the modeling of the EL region of GPCRs (Cavasotto *et al.*, 2015), the most speculative part of the model corresponds to the loop regions of the receptor and their potential interactions with the N-terminal fragment of the natural agonist. On the other side, we found that the binding mode of the common amidated C-terminus was almost identical for PYY and the four truncated analogs, in particular around the ^{32}TRQRY^{36}-NH_2 motif, while truncations of the proline helix mainly affected the folding of the peptides. This would explain the gradual, smooth affinity loss of truncations up to residue 18, while PYY-(22-36) exhibited a larger reduction of affinity, in agreement with earlier studies on NPY truncations (Kaiser and Kézdy, 1983; Fuhlendorff *et al.*, 1990). Our simulations indicate that the interactions between the α-helix and the proline-helix region are critical to maintain the PP-fold, characteristic of all Y-receptor agonist peptides (Glover *et al.*, 1984; Bjørnholm *et al.*, 1993; Nygaard *et al.*, 2006). PYY-(3-36) also maintains this fold, as revealed in NMR studies (Nygaard *et al.*, 2006), but more severe truncations of the peptide lead to misfolding, in line with the experimental data available (Minakata and Iwashita, 1990; Hu *et al.*, 1994). Taken together, our binding affinity data and the subsequent MD analysis support the current model for Y_2 agonism, where the activation trigger is located in the amidated C-terminus fragment. The function of the remaining peptide

Molecular Pharmacology Fast Forward. Published on January 24, 2018 as DOI: 10.1124/mol.117.110627
This article has not been copyedited and formatted. The final version may differ from this version.

might be related to the kinetics of peptide binding, as earlier indicated for NPY (Fuhlendorff *et al.*, 1990). While intriguing, this point should be investigated with further kinetic experiments of the binding of different peptides.

The pattern of interactions derived from our MD analysis for the ^{32}TRQRY^{36}-NH_2 motif with hY_2 was essentially the same as proposed in our earlier study (Xu *et al.*, 2013). While many of these interactions were further supported by existing mutagenesis data, either previously reported or designed and tested in that study (Fig. 2), we herein investigated novel potential interactions with receptor mutagenesis and peptide modifications. Position T^{32} in the peptide is predicted close to Phe307$^{7.35}$, which was confirmed by the experimental data: while the alanine mutant of this residue had a moderate impact on affinity of the peptide, this was partially recovered for the (T^{32}A)PYY-(3-36) peptide analog, which otherwise showed lower affinity for the WT-Y_2 receptor. Conversely, the corresponding introduction of an aromatic sidechain in the peptide, i.e. (T^{32}F)PYY-(3-36) analog, was better tolerated by the WT-Y_2 receptor suggesting a π-stacking interaction in the peptide mutant. The proximity of position Phe307$^{7.35}$ with residue T^{32} in the peptide is in contrast with the previous suggestion of an interaction of T^{32} with Tyr110$^{2.64}$, a possibility that we could rule out based on the minor effect of peptide binding of the corresponding Tyr110$^{2.64}$Ala mutant.

The pair of arginines in the C-terminal tail of the peptide (R^{33} and R^{35}) are involved in salt-bridge interactions with Glu205$^{5.24}$ and Asp292$^{6.59}$, as independently proposed in the most recent models of agonist-Y_2 receptor binding (Xu *et al.*, 2013; Kaiser *et al.*, 2015). The glutamine residue in between this arginine pair (Q^{34}) protrudes in the opposite direction, facing receptor residues Gln130$^{3.32}$ and Thr111$^{2.65}$. This interaction pattern is supported by our previous and current site-directed

Molecular Pharmacology Fast Forward. Published on January 24, 2018 as DOI: 10.1124/mol.117.110627
This article has not been copyedited and formatted. The final version may differ from this version.

mutagenesis data. Mutations of Thr111$^{2.65}$ were here combined with the Q^{34}L peptide analog, the results suggesting a smooth interaction between the two positions. Thus, residue Gln130$^{3.32}$ appears to be the main anchoring point for Q^{34}, in line with the high sensibility to peptide binding of conservative mutations (His, Glu) of this position. (Xu *et al.*, 2013). We found further evidence for this interpretation in our FEP calculations of the Gln130$^{3.32}$Glu and Gln130$^{3.32}$His mutants. This is in contrast with the alternative role proposed for this residue in the model from Beck-Sickinger and co-workers, where this residue is the anchoring point of the amidated C-terminus (Kaiser *et al.*, 2015). In addition, Gln130$^{3.32}$ might have a structural role by participating in a network of interhelical interactions with Thr107$^{2.61}$ and His311$^{7.39}$, supported by the lack of receptor expression in the corresponding Ala and Leu mutants (Xu *et al.*, 2013). Our model, on the other hand, suggests a direct interaction between Y^{36} and Leu284$^{6.51}$. This is in line with our previous data that showed an increased binding affinity for the Leu284$^{6.51}$Tyr mutant, indicative of a possible π-stacking of the aromatic rings. This would indeed leave the amidated C-terminal group exposed to more diffuse polar interactions with Gln288$^{6.55}$ and Tyr219$^{5.38}$. This possibility was thoroughly investigated here by receptor mutants, combined with peptide modifications on the C-terminal amide group, and the results interpreted with FEP simulations of the generated mutants. For mutations at these two positions, our FEP calculations consistently reproduce the small to moderate effect observed when removing the sidechain (Gln288$^{6.55}$Ala, Tyr219$^{5.38}$Ala), replacing it with an apolar side chain (Leu mutants) or even the small effects of more conservative mutants like Gln288$^{6.55}$Asn/Glu. On the other hand, the introduction of a flexible and positively charged arginine in Gln288$^{6.55}$ was not tolerated by our model, in clear agreement with the experimental data on that mutant. Additional verification of this polar

network was given by the conspicuous loss of binding affinity observed for the peptide modifications of the amidated C-terminus. To further test the binding mode proposed, we designed three mutants that would be expected to hinder the peptide to go into the binding pocket: Pro127$^{3.29}$Ala, Pro127$^{3.29}$Leu and Cys103$^{2.57}$Phe. All three of these exhibited too low affinities to be measured, precisely, but potencies could be determined accurately. This confirmed our hypothesis that Pro$^{3.29}$ is key to maintain the integrity of the binding pocket in the upper side of the TM2-TM3 region, where Cys103$^{2.57}$Phe could act as an obstacle at the Y^{36} binding pocket.

We repeatedly found that single-amino acid replacements had a greater impact in the peptides than in the receptors. The reason for this is probably that the receptor has multiple points of interaction with each residue in the peptide. A given peptide residue is usually surrounded by, and interacts with, many receptor residues. Each receptor residue would thereby contribute relatively little to the interactions with the peptide. For the peptide, on the other hand, the number of residues that interact with the receptor is more limited, meaning that each one makes a greater contribution to receptor binding.

Another important aspect is that most of the identified residues that are involved in the pentapeptide interactions are highly conserved among NPY family receptor subtypes and also the more distantly related RFamide receptors in human and other vertebrates. This suggests that the binding modes of these receptors share structural similarities, reflecting their common evolutionary ancestry. Furthermore, the binding pockets formed by these conserved residues in the NPY-family receptors are likely to explain the conservation of the C-terminus of the NPY family peptides. The positions that differ between peptide-binding receptors for peptides ending with RFamide, rather than the RYamide of PYY and NPY, are likely to contribute to peptide-receptor

Molecular Pharmacology Fast Forward. Published on January 24, 2018 as DOI: 10.1124/mol.117.110627
This article has not been copyedited and formatted. The final version may differ from this version.

preferences. This information may be utilized for synthesis of Y_2-selective agonists. It is important to take into consideration that some of the positions in the peptides and receptors may be subjected to negative selection pressures to avoid cross-binding to other members of these families.

Our study presents a unique combination of computational and in vitro pharmacological analyses, focused on the effect on ligand binding of both receptor mutagenesis and peptide modifications. This broad approach allowed us to deduce a more detailed model for the interactions of the native PYY agonist with the human Y_2 receptor. By also including evolutionary comparisons of the critical positions, we have identified several positions that are likely to be important for PYY binding to Y_2 and are also likely to be involved in PYY binding to the other NPY-family receptor subtypes. The interaction pattern described between ^{32}TRQRY^{36}-NH_2 and hY_2 may guide the optimization of Y_2-selective agonists, with potential applications in the control of appetite.

Authorship Contributions:

Participated in Research Design: B.X., D.L., H.G.d.T., B.S.W., S.Ø.

Conducted Experiments: B.X., S.Ø., J.P, J.F.P.

Performed Calculations: S.V.

Performed Data Analysis: B.X., S.V., J.Å., H.G.d.T., D.L.

Wrote or contributed to the writing of the manuscript: H.G.d.T., D.L., S.V., B.X., B.S.W., S.Ø., J.F.P., J.Å.

References

Åkerberg H, Fällmar H, Sjödin P, Boukharta L, Gutiérrez-de-Terán H, Lundell I, Mohell N, and Larhammar D (2010) Mutagenesis of human neuropeptide Y/peptide YY receptor Y2 reveals additional differences to Y1 in interactions with highly conserved ligand positions. *Regul Pept* **163**:120–129.

Albertsen L, Andersen JJ, Paulsson JF, Thomsen JK, Norrild JC, and Strømgaard K (2013) Design and Synthesis of Peptide YY Analogues with C-terminal Backbone Amide-to-Ester Modifications. *ACS Med Chem Lett* **4**:1228–1232.

Åqvist J (1996) Calculation of absolute binding free energies for charged ligands and effects of long-range electrostatic interactions. *J Comput Chem* **17**:1587–1597.

Balasubramaniam A, Tao Z, Zhai W, Stein M, Sheriff S, Chance WT, Fischer JE, Eden PE, Taylor JE, Liu CD, McFadden DW, Voisin T, Roze C, and Laburthe M (2000) Structure-activity studies including a Ψ(CH2-NH) scan of peptide YY (PYY) active site, PYY(22-36), for interaction with rat intestinal PYY receptors: Development of analogues with potent in vivo activity in the intestine. *J Med Chem* **43**:3420–3427.

Ballesteros JA, and Weinstein H (1995) [19] Integrated methods for the construction of three-dimensional models and computational probing of structure-function relations in G protein-coupled receptors. *Methods Neurosci* **25**:366–428.

Beck-Sickinger AG, Weland HA, Wittneben H, Willim KDD, Rudolf K, and Jung G (1994) Complete L-Alanine Scan of Neuropeptide Y Reveals Ligands Binding to Y1 and Y2 Receptors with Distinguished Conformations. *Eur J Biochem* **225**:947–958.

Berger O, Edholm O, and Jahnig F (1997) Molecular Dynamics Simulations of a Fluid Bilayer of Dipalmitoylphosphatidylcholine at Full Hydration, Constant

Pressure, and Constant Temperature. *Biophys J* **72**:2002–2013.

Bjørnholm B, Jørgensen FS, and Schwartz TW (1993) Conservation of a helix-stabilizing dipole moment in the PP-fold family of regulatory peptides. *Biochemistry* **32**:2954–2959.

Boukharta L, Gutiérrez-de-Terán H, Åqvist J, Impey R, and Klein M (2014) Computational Prediction of Alanine Scanning and Ligand Binding Energetics in G-Protein Coupled Receptors. *PLoS Comput Biol* **10**:e1003585, Public Library of Science.

Boyle RG, Downham R, Ganguly T, Humphries J, Smith J, and Travers S (2005) Structure-activity studies on prolactin-releasing peptide (PrRP). Analogues of PrRP-(19-31)-peptide. *J Pept Sci* **11**:161–165.

Brothers SP, and Wahlestedt C (2010) Therapeutic potential of neuropeptide Y (NPY) receptor ligands. *EMBO Mol Med* **2**:429–439.

Cavasotto CN, Palomba D, Pierce KL, and Al E (2015) Expanding the horizons of G protein-coupled receptor structure-based ligand discovery and optimization using homology models. *Chem Commun* **51**:13576–13594.

Degen L, Oesch S, Casanova M, Graf S, Ketterer S, Drewe J, and Beglinger C (2005) Effect of peptide YY3-36 on food intake in humans. *Gastroenterology* **129**:1430–1436.

Ehrlich GK, Michel H, Truitt T, Riboulet W, Pop-Damkov P, Goelzer P, Hainzl D, Qureshi F, Lueckel B, Danho W, Conde-Knape K, and Konkar A (2013) Preparation and characterization of albumin conjugates of a truncated peptide YY analogue for half-life extension. *Bioconjug Chem* **24**:2015–2024.

Elphick MR, and Mirabeau O (2014) The evolution and variety of RFamide-type neuropeptides: Insights from deuterostomian invertebrates. *Front Endocrinol*

(Lausanne) **5**:1–11.

Estep KG, Neipp CE, Stramiello LMS, Adam MD, Allen MP, Robinson S, and Roskamp EJ (1998) Indole Resin: A Versatile New Support for the Solid-Phase Synthesis of Organic Molecules. *J Org Chem* **63**:5300–5301.

Fällmar H, Åkerberg H, Gutiérrez-de-Terán H, Lundell I, Mohell N, and Larhammar D (2011) Identification of positions in the human neuropeptide Y/peptide YY receptor Y2 that contribute to pharmacological differences between receptor subtypes. *Neuropeptides* **45**:293–300.

Fekete C, Sarkar S, Rand WM, Harney JW, Emerson CH, Bianco AC, Beck-Sickinger A, and Lechan RM (2002) Neuropeptide Y1 and Y5 receptors mediate the effects of neuropeptide Y on the hypothalamic-pituitary-thyroid axis. *Endocrinology* **143**:4513–4519.

Findeisen M, Würker C, Rathmann D, Meier R, Meiler J, Olsson R, and Beck-Sickinger AG (2012) Selective mode of action of guanidine-containing non-peptides at human NPFF receptors. *J Med Chem* **55**:6124–6136.

Fuhlendorff J, Langeland Johansen N, Melberg SG, Thogersen H, and Schwartz TW (1990) The antiparallel pancreatic polypeptide fold in the binding of neuropeptide Y to Y1 and Y2 receptors. *J Biol Chem* **265**:11706–11712.

Glover ID, Barlow DJ, Pitts JE, Wood SP, Tickle IJ, Blundell TL, Tatemoto K, Kimmel JR, Wollmer A, Strassburger W, and Zhang Y‐S (1984) Conformational studies on the pancreatic polypeptide hormone family. *Eur J Biochem* **142**:379–385.

Gutiérrez-de-Terán H, Bello X, and Rodríguez D (2013) Characterization of the dynamic events of GPCRs by automated computational simulations. *Biochem Soc Trans* **41**:205–212.

Hess B, Kutzner C, van der Spoel D, and Lindahl E (2008) GROMACS 4: Algorithms for Highly Efficient, Load-Balanced, and Scalable Molecular Simulation. *J Chem Theory Comput* **4**:435–447.

Hu L, Balse P, and Doughty MB (1994) Neuropeptide Y N-terminal deletion fragments: Correlation between solution structure and receptor binding activity at Y1 receptors in rat brain cortex. *J Med Chem* **37**:3622–3629.

Humphrey W, Dalke A, and Schulten K (1996) VMD: Visual molecular dynamics. *J Mol Graph* **14**:33–38.

Kaiser A, Müller P, Zellmann T, Scheidt HA, Thomas L, Bosse M, Meier R, Meiler J, Huster D, Beck-Sickinger AG, and Schmidt P (2015) Unwinding of the C-Terminal Residues of Neuropeptide Y is critical for Y2 Receptor Binding and Activation. *Angew Chemie Int Ed* **54**:7446–7449.

Kaiser ET, and Kézdy FJ (1983) Secondary structures of proteins and peptides in amphiphilic environments. (A review). *Proc Natl Acad Sci U S A* **80**:1137–1143.

Kaminski GA, Friesner RA, Tirado-rives J, and Jorgensen WL (2001) Evaluation and Reparametrization of the OPLS-AA Force Field for Proteins via Comparison with Accurate Quantum Chemical Calculations on Peptides †. *J Phys Chem B* **105**:6474–6487.

Kannoa T, Kanatani A, Keen SLC, Arai-Otsuki S, Haga Y, Iwama T, Ishihara A, Sakuraba A, Iwaasa H, Hirose M, Morishima H, Fukami T, and Ihara M (2001) Different binding sites for the neuropeptide Y Y1 antagonists 1229U91 and J-104870 on human Y1 receptors. *Peptides* **22**:405–413.

Katritch V, Cherezov V, and Stevens RC (2013) Structure-Function of the G Protein–Coupled Receptor Superfamily. *Annu Rev Pharmacol Toxicol* **53**:531–556.

Keränen H, Åqvist J, and Gutiérrez-de-Terán H (2015) Free energy calculations of

A2A adenosine receptor mutation effects on agonist binding. *Chem Commun* **51**:3522–3525, Royal Society of Chemistry.

Keränen H, Gutiérrez-de-Terán H, and Åqvist J (2014) Structural and energetic effects of A2A adenosine receptor mutations on agonist and antagonist binding. *PLoS One* **9**:e108492.

King G, and Warshel A (1989) A surface constrained all-atom solvent model for effective simulations of polar solutions. *J Chem Phys* **91**:3647.

Kirby DA, Britton KT, Aubert ML, and Rivier JE (1997) Identification of High-Potency Neuropeptide Y Analogues through Systematic Lactamization. *J Med Chem* **40**:210–215.

Kostenis E (2002) Potentiation of GPCR-signaling via membrane targeting of G Protein α Subunits. *J Recept Signal Transduct* **22**:267–281.

Kristiansen K (2004) Molecular mechanisms of ligand binding, signaling, and regulation within the superfamily of G-protein-coupled receptors: molecular modeling and mutagenesis approaches to receptor structure and function. *Pharmacol Ther* **103**:21–80.

Larhammar D, Xu B, and Bergqvist CA (2014) Unexpected multiplicity of QRFP receptors in early vertebrate evolution. *Front Neurosci* **8**:1–6.

Laskowski RA, MacArthur MW, Moss DS, and Thornton JM (1993) PROCHECK: a program to check the stereochemical quality of protein structures. *J Appl Crystallogr* **26**:283–291, International Union of Crystallography.

Le Marec O, Neveu C, Lefranc B, Dubessy C, Boutin JA, Do-Régo JC, Costentin J, Tonon MC, Tena-Sempere M, Vaudry H, and Leprince J (2011) Structure-activity relationships of a series of analogues of the RFamide-related peptide 26RFa. *J Med Chem* **54**:4806–4814.

Lecklin A, Lundell I, Paananen L, Wikberg JES, Männistö PT, and Larhammar D (2002) Receptor subtypes Y1 and Y5 mediate neuropeptide Y induced feeding in the guinea-pig. *Br J Pharmacol* **135**:2029–2037.

Lee FS, and Warshel A (1992) A local reaction field method for fast evaluation of long‐range electrostatic interactions in molecular simulations. *J Chem Phys* **97**:3100–3107.

Marelius J, Kolmodin K, Feierberg I, and Åqvist J (1998) Q: a molecular dynamics program for free energy calculations and empirical valence bond simulations in biomolecular systems. *J Mol Graph Model* **16**:213–225.

Mashiko S, Moriya R, Ishihara A, Gomori A, Matsushita H, Egashira S, Iwaasa H, Takahashi T, Haga Y, Fukami T, and Kanatani A (2009) Synergistic interaction between neuropeptide Y1 and Y5 receptor pathways in regulation of energy homeostasis. *Eur J Pharmacol* **615**:113–117, Elsevier B.V.

Mauduit C, Gasnier F, Rey C, Chauvin M a, Stocco DM, Louisot P, and Benahmed M (1998) Tumor necrosis factor-alpha inhibits leydig cell steroidogenesis through a decrease in steroidogenic acute regulatory protein expression. *Endocrinology* **139**:2863–2868.

McGibbon RT, Beauchamp KA, Harrigan MP, Klein C, Swails JM, Hernández CX, Schwantes CR, Wang LP, Lane TJ, and Pande VS (2015) MDTraj: A Modern Open Library for the Analysis of Molecular Dynamics Trajectories. *Biophys J* **109**:1528–1532.

Merten N, Lindner D, Rabe N, Römpler H, Mörl K, Schöneberg T, and Beck-Sickinger AG (2007) Receptor subtype-specific docking of Asp6.59 with C-terminal arginine residues in Y receptor ligands. *J Biol Chem* **282**:7543–7551, American Society for Biochemistry and Molecular Biology.

Michel MC, Beck-Sickinger A, Cox H, Doods HN, Herzog H, Larhammar D, Quirion R, Schwartz T, and Westfall T (1998) XVI. International Union of Pharmacology Recommendations for the Nomenclature of Neuropeptide Y, Peptide YY, and Pancreatic Polypeptide Receptors. *Pharmacol Rev* **50**:143–150.

Minakata H, and Iwashita T (1990) Synthesis of analogues of peptide YY with modified N-terminal regions: Relationships of amphiphilic secondary structures and activity in rat vas deferens. *Biopolymers* **29**:61–67, Wiley Subscription Services, Inc., A Wiley Company.

Monks S a, Karagianis G, Howlett GJ, and Norton RS (1996) Solution structure of human neuropeptide Y. *J Biomol NMR* **8**:379–390.

Neary MT, and Batterham RL (2009) Peptide YY: Food for thought. *Physiol Behav* **97**:616–619, Elsevier Inc.

Nishizawa N, Niida A, Masuda Y, Kumano S, Yokoyama K, Hirabayashi H, Amano N, Ohtaki T, and Asami T (2017) Antiobesity effect of a short-length peptide YY analogue after continuous administration in mice. *ACS Med Chem Lett* **8**:628–631.

Nøhr AC, Jespers W, Shehata MA, Floryan L, Isberg V, Andersen KB, Åqvist J, Gutiérrez-de-Terán H, Bräuner-Osborne H, and Gloriam DE (2017) The GPR139 reference agonists 1a and 7c, and tryptophan and phenylalanine share a common binding site. *Sci Rep* **7**:1128.

Nosé S, and Klein ML (1983) Constant pressure molecular dynamics for molecular systems. *Mol Phys* **50**:1055–1076, Taylor & Francis Group .

Nygaard R, Nielbo S, Schwartz TW, and Poulsen FM (2006) The PP-Fold Solution Structure of Human Polypeptide YY and Human PYY3-36 As Determined by NMR. *Biochemistry* **45**:8350–8357.

Pedersen SL, Holst B, Vrang N, and Jensen KJ (2009) Modifying the conserved C-terminal tyrosine of the peptide hormone PYY3-36 to improve Y2 receptor selectivity. *J Pept Sci* **15**:753–759.

Pedersen SL, Sasikumar PG, Chelur S, Holst B, Artmann A, Jensen KJ, and Vrang N (2010) Peptide hormone isoforms: N-terminally branched PYY3-36 isoforms give improved lipid and fat-cell metabolism in diet-induced obese mice. *J Pept Sci* **16**:664–673.

Pedragosa-Badia X, Sliwoski GR, Nguyen ED, Lindner D, Stichel J, Kaufmann KW, Meiler J, and Beck-Sickinger AG (2014) Pancreatic polypeptide is recognized by two hydrophobic domains of the human Y4 receptor binding pocket. *J Biol Chem* **289**:5846–5859.

Pedragosa-Badia X, Stichel J, and Beck-Sickinger AG (2013) Neuropeptide y receptors: How to get subtype selectivity. *Front Endocrinol (Lausanne)* **4**:1–13.

Roland BL, Sutton SW, Wilson SJ, Luo L, Pyati J, Huvar R, Erlander MG, and Lovenberg TW (1999) Anatomical distribution of prolactin-releasing peptide and its receptor suggests additional functions in the central nervous system and periphery. *Endocrinology* **140**:5736–5745.

Ryckaert JP, Ciccotti G, and Berendsen HJC (1977) Numerical integration of the cartesian equations of motion of a system with constraints: molecular dynamics of n-alkanes. *J Comput Phys* **23**:327–341.

Salon JA, Lodowski DT, and Palczewski K (2011) The Significance of G Protein-Coupled Receptor Crystallography for Drug Discovery. *Pharmacol Rev* **63**:901–937.

Sato N, Ogino Y, Mashiko S, and Ando M (2009) Modulation of neuropeptide Y receptors for the treatment of obesity. *Expert Opin Ther Pat* **19**:1401–1415.

Sautel M, Rudolf K, Wittneben H, Herzog H, Martinez R, Munoz M, Eberlein W, Engel W, Walker P, and Beck-Sickinger AG (1996) Neuropeptide Y and the nonpeptide antagonist BIBP 3226 share an overlapping binding site at the human Y1 receptor. *Mol Pharmacol* **50**:285–292.

Schneeberger M, Gomis R, and Claret M (2014) Hypothalamic and brainstem neuronal circuits controlling homeostatic energy balance. *J Endocrinol* **220**:T25–T46.

Sherman W, Day T, Jacobson MP, Friesner RA, and Farid R (2006) Novel Procedure for Modeling Ligand/Receptor Induced Fit Effects. *J Med Chem* **49**:534–553.

Sjödin P, Holmberg SKS, Åkerberg H, Berglund MM, Mohell N, and Larhammar D (2006) Re-evaluation of receptor–ligand interactions of the human neuropeptide Y receptor Y1: a site-directed mutagenesis study. *Biochem J* **393**:161–169.

Vasile S, Esguerra M, Jespers W, Oliveira A, Sallander J, Åqvist J, and Gutiérrez-de-Terán H (2017) Characterization of ligand binding to GPCRs through computational methods., in *Computational Methods for GPCR Drug Discovery* p in press.

Walther C, Mörl K, and Beck-Sickinger AG (2011) Neuropeptide Y receptors: Ligand binding and trafficking suggest novel approaches in drug development. *J Pept Sci* **17**:233–246.

White JF, Noinaj N, Shibata Y, Love J, Kloss B, Xu F, Gvozdenovic-Jeremic J, Shah P, Shiloach J, Tate CG, and Grisshammer R (2012) Structure of the agonist-bound neurotensin receptor. *Nature* **490**:508–513.

Xu B, Fällmar H, Boukharta L, Pruner J, Lundell I, Mohell N, Gutiérrez-de-Terán H, Åqvist J, and Larhammar D (2013) Mutagenesis and Computational Modeling of Human G-Protein-Coupled Receptor Y2 for Neuropeptide Y and Peptide YY.

Biochemistry **52**:7987–7998.

Yulyaningsih E, Zhang L, Herzog H, and Sainsbury A (2011) NPY receptors as potential targets for anti-obesity drug development. *Br J Pharmacol* **163**:1170–1202.

Yun S, Kim DK, Furlong M, Hwang JI, Vaudry H, and Seong JY (2014) Does kisspeptin belong to the proposed RF-amide peptide family? *Front Endocrinol (Lausanne)* **5**:22–26.

Zhang L, Bijker MS, and Herzog H (2011) The neuropeptide y system: Pathophysiological and therapeutic implications in obesity and cancer. *Pharmacol Ther* **131**:91–113, Elsevier Inc.

Zhukov A, Andrews SP, Errey JC, Robertson N, Tehan B, Mason JS, Marshall FH, Weir M, and Congreve M (2011) Biophysical Mapping of the Adenosine A2A Receptor. *J Med Chem* **54**:4312–4323.

Molecular Pharmacology Fast Forward. Published on January 24, 2018 as DOI: 10.1124/mol.117.110627
This article has not been copyedited and formatted. The final version may differ from this version.

Footnotes

This work was supported by a postdoctoral fellowship for B. X. from Novo Nordisk A/S, DK-2880 Bagsvaerd, Denmark, the Swedish Research Council (Department of Cell and Molecular Biology, Grant 521-2014-2118) and the Swedish Strategic Research Program eSSENCE. The computations were performed on resources provided by the Swedish National Infrastructure for Computing (SNIC).

Molecular Pharmacology Fast Forward. Published on January 24, 2018 as DOI: 10.1124/mol.117.110627
This article has not been copyedited and formatted. The final version may differ from this version.

Legends for Figures

Figure 1. The binding mode of the amidated C-terminus of PYY and four truncated analogues in human Y_2: A) WT-PYY; B) PYY-(3-36); C) PYY-(18-36); D) PYY-(19-36); E) PYY-(22-36). The interacting residues were selected on the basis of hydrogen bonds occurring at least 40% of the time in each replicate of the MD simulations (Supplemental Table 1) or C_α- C_α distances under 9 Å.

Figure 2. Proposed binding mode of ^{32}TRQRY^{36}-NH_2 to the hY_2 receptor, with the receptor residues participating ligand binding and studied by site-directed mutagenesis denoted in sticks and labelled in bold. The effect in fold change in agonist affinity (or potency, indicated by [a]) is indicated for mutations reported in references (Xu *et al.* 2013, Merten *et al.* 2007), where (nb) indicates no detectable binding. Residues selected for mutagenesis in this study are indicated in red, and the corresponding results reported in Table 2.

Figure 3: Affinity values (pK_i = –Log Conc (M), Y axis) of PYY-(3-36) analogues for WT-hY_2 and its mutants. The upper panels depict data for peptide modifications on position T^{32} (T^{32}A, T^{32}F) and Q^{34} (Q^{34}L). Lower panels refer to modifications on the amidated C-terminus, replaced by three different chemical groups ($NHCH_3$, COOH, CH_2OH). Within each panel, affinity for a given mutant (indicated by three-letter amino acid code) is given for PYY-(3-36) or the corresponding peptide modification (indicated in parenthesis). Error bars indicate SEM. The statistical significance of pairwise comparison is indicated with asterisks following the code: *: $p<0.05$, **: $p < 0.01$, ***: $p < 0.001$.

Molecular Pharmacology Fast Forward. Published on January 24, 2018 as DOI: 10.1124/mol.117.110627
This article has not been copyedited and formatted. The final version may differ from this version.

Figure 4: Calculated and experimental relative binding free energies (ΔΔG, kcal/mol) for PYY-(3-36) to nine selected hY_2 mutants compared to WT-hY_2. Black bars indicate $\Delta\Delta G_{bind}^{exp}$ (values from Table 2 and (*) from Bo et al., Biochemistry 2013), grey bars represent $\Delta\Delta G_{bind}^{FEP}$ (values from Supplemental Table 4). The standard error of the mean (SEM) is shown with error bars (calculated from 10 independent replica simulations for the FEP binding free energies, or from 3 independent experiments for the experimental data).

Figure 5. Alignment of human NPY family receptors and RF amide receptors. The Y_2 transmembrane regions have been marked with frames based on the transmembrane region prediction of GPCRDB. The residues selected for mutagenesis were marked with light grey, and the most conserved position in each helix (TM.50, according to Ballesteros-Weinstein) is highlighted in dark grey.

Molecular Pharmacology Fast Forward. Published on January 24, 2018 as DOI: 10.1124/mol.117.110627
This article has not been copyedited and formatted. The final version may differ from this version.

Tables

Table 1. Binding affinities of PYY and its truncated analogues for WT-hY_2

Peptide	WT-hY_2		Fold change	n
	K_i (nM)[a,b]	95% CI[c]	K_i / PYY-(3-36) K_i	
PYY	0.057*	0.042; 0.078	0.15	22
PYY-(3-36)	0.38	0.31; 0.44	1	43
PYY-(18-36)	1.4 *	0.78; 2.4	3.6	6
PYY-(19-36)	1.8*	0.96; 3.4	4.8	6
PYY-(22-36)	9.6*	4.7; 19	25	5

a) K_i is calculated as the geometric mean of the n independent experiments. b) One-way ANOVA with Dunnett post hoc analysis was performed for the pK_i values, the significance of the differences with PYY-(3-36) is indicated (*: $p < 0.001$). c) 95% confidence interval (CI), given as [lower; upper].

Molecular Pharmacology Fast Forward. Published on January 24, 2018 as DOI: 10.1124/mol.117.110627
This article has not been copyedited and formatted. The final version may differ from this version.

Table 2. Binding affinities or potencies of PYY-(3-36) for WT-hY_2 and mutants

Y_2 and mutants	PYY-(3-36) K_i / *EC50* (nM)[a, b]	PYY-(3-36) 95% CI[c]	Fold change (WT / mut)	n
WT-hY2	0.38	0.31; 0.44	1	43
	0.31[a]	0.25; 0.38	1	5
Cys103$^{2.57}$Phe[a]	*73***	18; 283	235	3
Tyr110$^{2.64}$Ala	1.4*	0.33; 5.6	3.6	3
Thr111$^{2.65}$Ala	12**	4.2; 37	33	3
Thr111$^{2.65}$Leu	0.54	0.095; 3.1	1.4	3
Pro127$^{3.29}$Ala[a]	*8.0***	0.35; 182	26	3
Pro127$^{3.29}$Leu[a]	*142***	43; 466	465	3
Arg187$^{4.64}$Ala	1.5**	0.92; 2.6	4.1	7
Glu188$^{4.65}$Ala	0.13	0.07; 0.29	0.3	4
Glu205$^{5.24}$Leu	8.5**	2.8; 26	23	3
Ser220$^{5.39}$Ala	2.2**	0.60; 8.3	5.9	3
Ser223$^{5.42}$Ala	0.55	0.15; 2.0	1.5	3
Ser223$^{5.42}$Leu	0.39	0.06; 2.6	1.0	3
Leu284$^{6.51}$Tyr	0.16	0.09; 0.29	0.4	3
His285$^{6.52}$Phe	0.10	0.03; 0.38	0.3	4
Gln288$^{6.55}$Ala	0.73	0.13; 4.3	1.9	3
Gln288$^{6.55}$Leu	1.3**	0.79; 2.2	3.5	7
Gln288$^{6.55}$Glu	1.0	0.15; 7.4	2.7	3
Gln288$^{6.55}$Arg	30**	18; 49	79	7
Tyr303$^{7.31}$Ala	0.77	0.40; 1.5	2	3
Phe307$^{7.35}$Ala	17**	8.4; 34	45	5

a) Affinity (K_i) or potency (EC_{50}, in italics) values are calculated as the geometric mean of the n independent experiments. b) One-way ANOVA with Dunnett post hoc analysis were used for pK_i, (or potency in pEC50, respectively). Asterisks indicate the statistical significance of differences of PYY-(3-36) affinity in pK_i, (or potency in pEC50, respectively) between Y_2 and its mutants (*: $p < 0.01$, **: $p < 0.001$). c) 95% confidence interval (CI), given as [lower; upper]

Molecular Pharmacology Fast Forward. Published on January 24, 2018 as DOI: 10.1124/mol.117.110627
This article has not been copyedited and formatted. The final version may differ from this version.

Figures

Figure 1

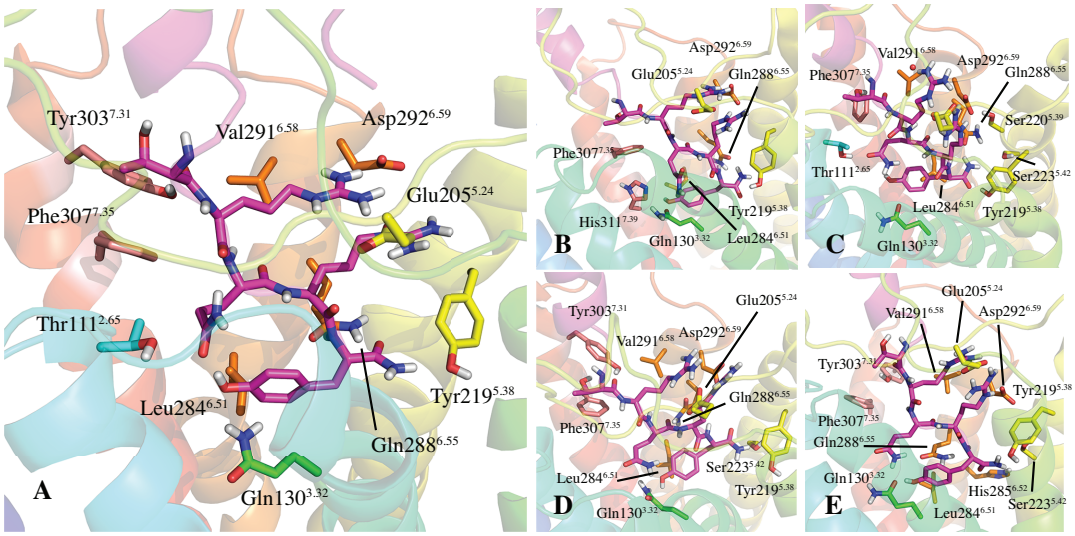

Molecular Pharmacology Fast Forward. Published on January 24, 2018 as DOI: 10.1124/mol.117.110627
This article has not been copyedited and formatted. The final version may differ from this version.

Figure 2

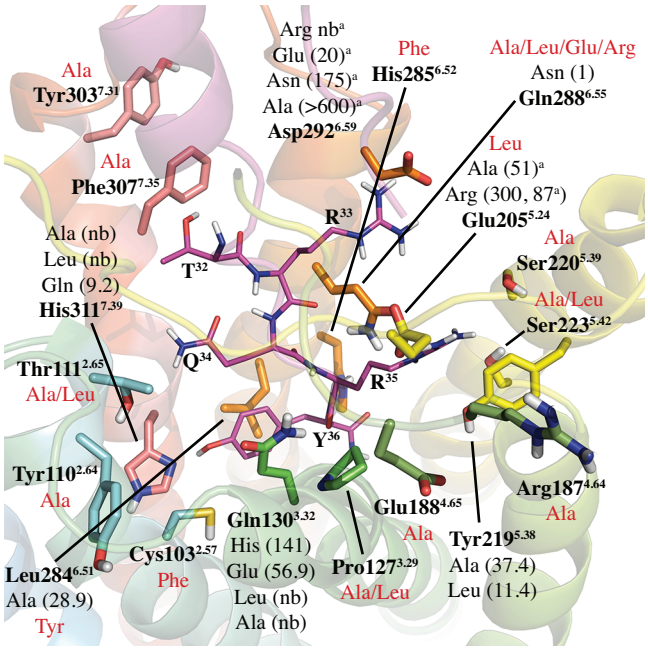

Molecular Pharmacology Fast Forward. Published on January 24, 2018 as DOI: 10.1124/mol.117.110627
This article has not been copyedited and formatted. The final version may differ from this version.

Figure 3

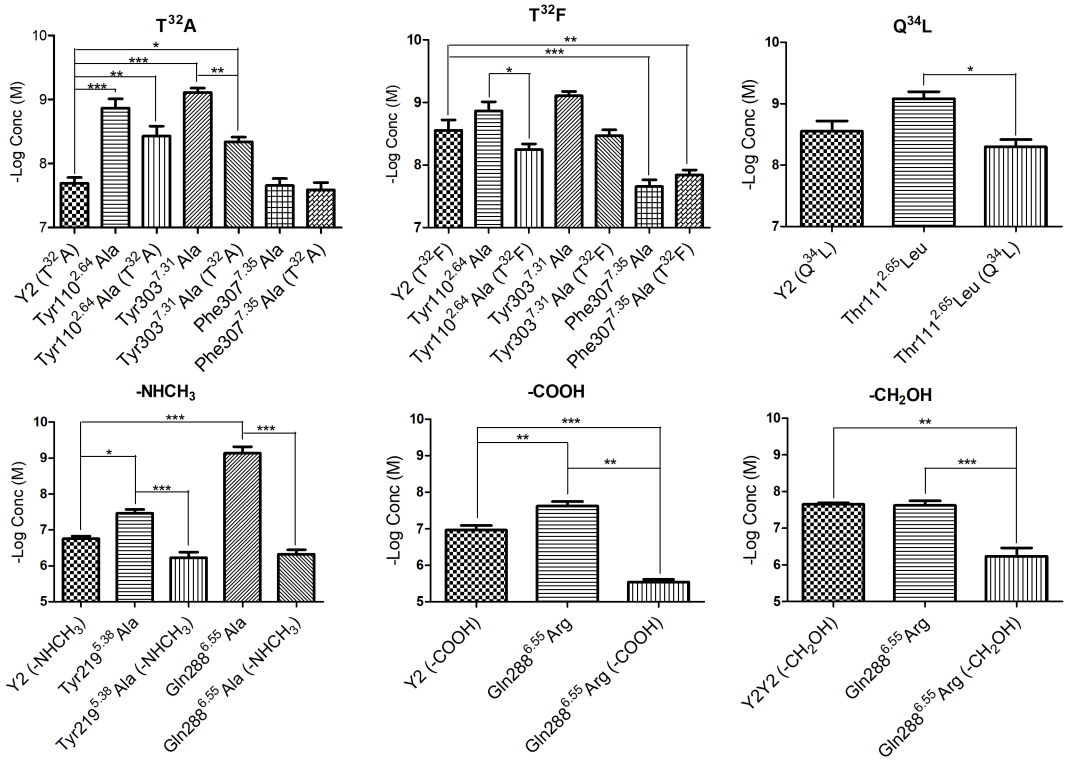

Molecular Pharmacology Fast Forward. Published on January 24, 2018 as DOI: 10.1124/mol.117.110627
This article has not been copyedited and formatted. The final version may differ from this version.

Figure 4

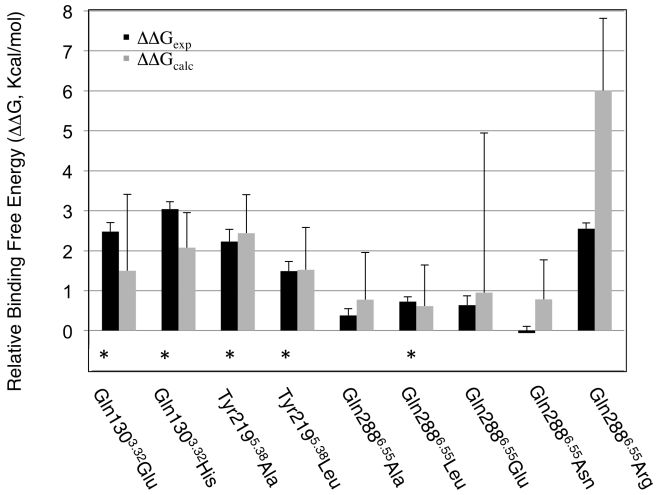

Molecular Pharmacology Fast Forward. Published on January 24, 2018 as DOI: 10.1124/mol.117.110627
This article has not been copyedited and formatted. The final version may differ from this version.

Figure 5